Antarct. Meteorite Res., **18**, 188–201, 2005

Comparative mineralogy of magmatic inclusions in olivine from the Chassigny and Nakhla martian meteorites

Akira Monkawa*, Takashi Mikouchi, Eisuke Koizumi and Masamichi Miyamoto

Department of Earth and Planetary Science, Graduate School of Science, University of Tokyo, Hongo, Bunkyo-ku, Tokyo 113-0033
**Corresponding author. E-mail: Monkawa.akira@nims.go.jp*

(Received March 11, 2004; Accepted January 13, 2005)

Abstract: Chassigny and Nakhla frequently contain magmatic inclusions in olivine. Some Al-, Ti-rich augites in Chassigny magmatic inclusions show reverse zoning from the Mg-poor core to the Mg-rich rim. This unique chemical zoning in Chassigny magmatic inclusion gives important implications for the crystallization of the magmatic inclusions. The crystallization stage of the Mg-poor core is different from that of the Mg-rich rim because the zoned augite has a sharp boundary between the Mg-rich and Mg-poor regions. The presence of such Al-, Ti-augite with reverse zoning implies that the bulk composition of the magmatic inclusion changed into Mg-rich. Such a compositional change of the magmatic inclusion can be produced by the melting of the surrounding olivine. There is a possibility that the melting of surrounding olivine has occurred during a shock event. In order to examine the possibility of the melting by a shock event, this study compared texture and constituent minerals of Chassigny magmatic inclusions with those of Nakhla magmatic inclusions. Although Chassigny magmatic inclusions have remarkable radial cracks around them, Nakhla magmatic inclusions only have ambiguous radial cracks. The presence of radial cracks in the Chassigny magmatic inclusion shows that the inclusions have been affected by a heavy impact event because cracks around magmatic inclusions formed by the fracturing of a phenocryst induced by rapid compression and decompression.

key words: martian meteorites, Chassigny, Nakhla, magmatic inclusion, reverse zoning

1. Introduction

Chassigny and Nakhla are members of the SNC (Shergottites-Nakhlites-Chassignite) meteorites that are widely believed to have originated from the planet Mars (*e.g.*, Wood and Ashwal, 1981; Bogard and Johnson, 1983; McSween, 1985, 1994). Chassigny is an igneous cumulate rock mainly composed of olivine (Fo_{68}). Nakhla is also an igneous cumulate rock mainly composed of augite with minor abundance of olivine. Olivine grains in Chassigny and Nakhla frequently contain magmatic inclusions (*e.g.*, Floran *et al.*, 1978; Treiman, 1993). Such magmatic inclusions are considered to give important information on the martian parent magma compositions and several attempts have been made to calculate the composition of the parent magma.

Longhi and Pan (1989) used mineral compositions of magmatic inclusions in

Chassigny and Nakhla and theoretical phase boundary relationships to constrain parent magma compositions. Johnson *et al*. (1991) estimated a Chassigny parent magma composition from mass balance calculations using magmatic inclusion phases. Nakhlite parent magmas have been modeled as simple mass balance mixtures of cumulus crystals plus interstitial liquid by Treiman (1993).

Although parent magma compositions of Chassigny and Nakhla have been estimated by several different studies as shown above, the crystallization process of constituent minerals in magmatic inclusions of Chassigny and Nakhla is not fully known. Furthermore, no discussion has been made of the possible compositional changes of the magmatic inclusions during crystallization of the host minerals and the effect of an impact event after the crystallization of the magmatic inclusion.

In this study, we describe Al-, Ti-rich augite with "reverse" chemical zoning in a Chassigny magmatic inclusion that has important implications for the crystallization conditions of the magmatic inclusions. We also compared texture and constituent minerals of Chassigny magmatic inclusions with those of Nakhla magmatic inclusions in order to understand the formation process of Chassigny magmatic inclusions in light of different degrees of shock metamorphism.

2. Samples and methods

2.1. Samples

In this study we analyzed five polished thin sections of martian meteorites. Three polished thin sections of Chassigny were analyzed (*ca*., 5×8 mm, *ca*., 4×6 mm and *ca*., 3×4 mm). The thin sections of Chassigny were supplied by the Smithsonian Institution, the University of Hawaii and the Natural History Museum of Berlin. Two thin sections (*ca*., 10×14 mm, respectively) were prepared from a Nakhla rock chip that was purchased from a meteorite dealer.

2.2. Electron microprobe analysis

Secondary electron images and backscattered electron (BSE) images were taken with a Hitachi S-4500 scanning electron microscope (SEM) equipped with an energy dispersive spectrometer (EDS) and KEVEX SIGMA analysis system. The accelerating voltage was 10–15 kV. The Hitachi SEM has a field emission gun (FEG-SEM) and is used to obtain high magnification BSE images up to 50000×. Elemental distribution maps and quantitative wavelength dispersive analyses were acquired by a JEOL JXA 8900L electron microprobe at the Ocean Research Institute of University of Tokyo. The accelerating voltage was 15 kV, and the beam current was 60–120 nA for mapping analyses. The element intensity at peak wavelength was measured for 15–30 ms for each pixel of the measured area. One pixel size of 1–20 μm was chosen. Quantitative microprobe analyses of most phases were obtained at 15 kV accelerating voltage with a beam current of 12 nA on a Faraday cage. Counting times at peak wavelengths were 20 s (10 s×2).

3. Results

3.1. Chassigny

Chassigny is a dunite with rare poikilitic low-Ca pyroxenes containing fine exsolution lamellae of high-Ca pyroxene (Johnson *et al*., 1991; Wadhwa and Crozaz, 1995). Olivine is 1–2 mm in size and occasionally shows 120° triple junctions at grain boundaries. The major element composition is homogeneous (Fo_{68}) as reported in previous studies (*e.g*., Floran *et al*., 1978). The olivine studied often contains magmatic inclusions also as reported by Floran *et al*. (1978).

We observed six magmatic inclusions in three thin sections of Chassigny. Magmatic inclusions studied are roughly divided into three types: polyphase inclusions, pure glass inclusions and monocrystalline (glass+crystal) inclusions (~50 μm) as reported by Varela *et al*. (2000). Most inclusions are surrounded by radial cracks in spite of the different types (Fig. 1).

Polyphase inclusions in Chassigny have variable sizes (20–150 μm in diameter) and contain euhedral to subhedral crystals in a glassy groundmass. The constituent phases are silica-rich glass, high-Ca pyroxene (Al-, Ti-rich augite), low-Ca pyroxene, kaersutite, chorapatite, pyrrhotite, chromite, pentlandite and biotite, but no feldspars as reported by Floran *et al*. (1978) and Johnson *et al*. (1991). We observed three polyphase inclusions (Fig. 1a; MI-A, Fig. 1b; MI-B, Fig. 1c; MI-C) in Chassigny olivines. These inclusions are mainly composed of Si-rich glass, high-Ca and low-Ca pyroxenes (Tables 1 and 2), and have reaction rims of low-Ca pyroxene surrounding the host olivine wall.

Both high-Ca and low-Ca pyroxenes are present in the Chassigny polyphase inclusions. In many cases, low-Ca pyroxenes are epitaxial to the host olivine along the polyphase inclusion boundary. The atomic $Fe^{2+}/(Fe^{2+}+Mg)$ ratios (Fe#) of the low-Ca pyroxenes are ~0.28. Low-Ca pyroxenes contain ~0.2 wt% TiO_2, ~0.2 wt% Cr_2O_3, and ~0.7 wt% Al_2O_3. Low-Ca pyroxenes have low wollastonite contents of ~5%. High-Ca pyroxenes are Ti- and Al-rich (TiO_2=1–2 wt%, Al_2O_3=4.5–7.5 wt%) with Fe# of ~0.24.

Some high-Ca pyroxenes in polyphase inclusions (MI-C) show reverse chemical zoning with Mg-rich rims (MgO=14 wt%) surrounding Mg-poor cores (MgO=10 wt%). The Fe# in the Mg-rich rim of this high-Ca pyroxene is 0.26 and that in the Mg-poor core of this high-Ca pyroxene is 0.35 (Fig. 2 and Table 3). Al_2O_3 and TiO_2 contents of the core are higher than those of the rim (Table 3). The boundary is sharp between the Mg-rich and Mg-poor regions (Fig. 3).

Two polyphase inclusions in the Chassigny thin sections studied contain euhedral kaersutite amphiboles (MI-A, B). The sizes of kaersutites are 50–80 μm. Kaersutites are in contact with low-Ca pyroxene, high-Ca pyroxene and Si-rich glass. On average, Chassigny kaersutites contain 7 wt% TiO_2 (Table 1). Their F and Cl abundances are low (F=0.5 wt%, Cl=0.1 wt%). Watson *et al*. (1994) determined the D/H ratio and water content of kaersutite grains in Chassigny by ion probe. The results show that these kaersutites have a high D/H ratio (δD=3000–4000‰) and low water content (0.1–0.2 wt%).

The opaque phases in the polyphase inclusions are mostly chromite and Fe sulfide.

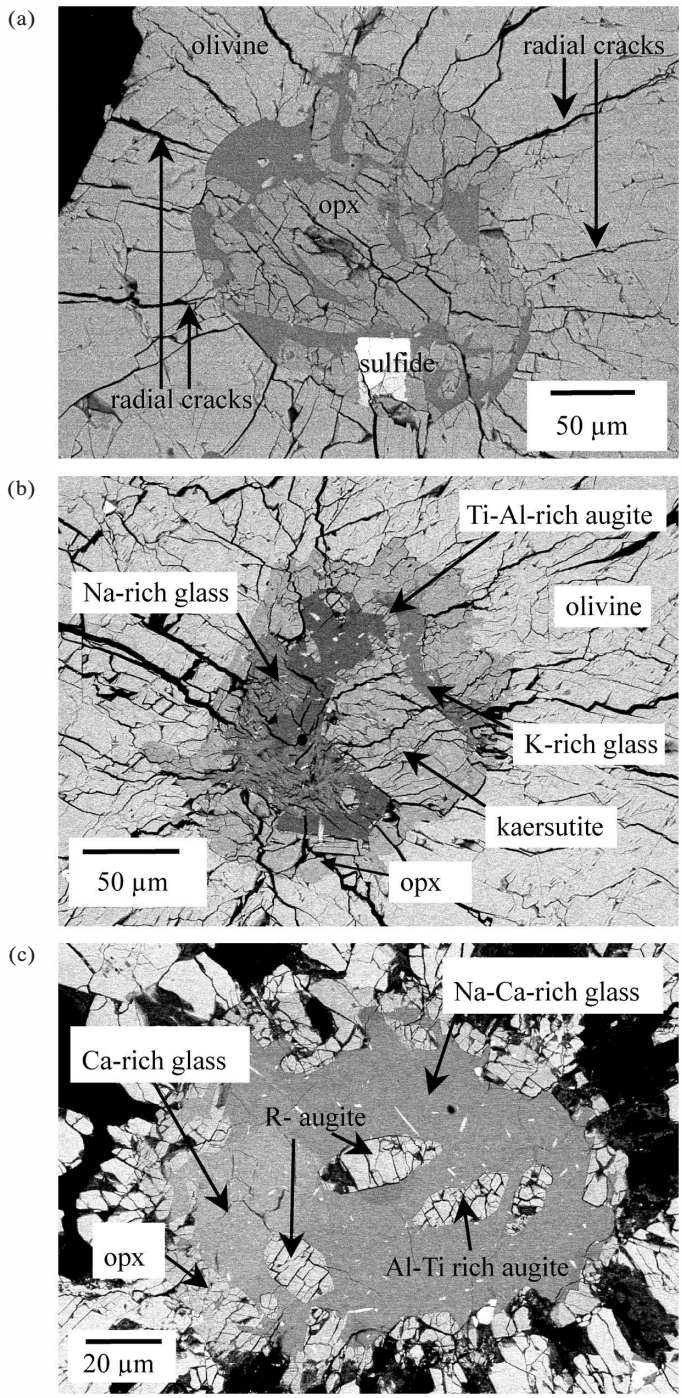

Fig. 1. (a) BSE image of a magmatic inclusion in Chassigny (MI-A). (b) BSE image of a polyphase inclusion (MI-B) in Chassigny olivine. (c) BSE image of a polyphase inclusion (MI-C) in Chassigny olivine. R-augite: reversely zoned augite.

Table 1. Chemical compositions of constituent minerals in the multi-crystalline magmatic inclusion (MI-B) with kaersutite in Chassigny olivine.

	MI-B					
	1	2	3	4	5	6
SiO_2	51.93	50.50	38.90	61.34	60.47	69.98
TiO_2	0.12	0.14	7.11	0.03	0.06	0.08
Al_2O_3	0.43	0.49	15.06	21.47	16.73	19.24
Cr_2O_3	0.07	0.04	0.20	-	0.01	-
FeO*	17.99	33.08	10.35	0.40	0.19	0.49
MnO	0.57	0.86	0.22	0.01	0.04	-
MgO	10.70	13.60	11.05	0.02	0.10	0.02
CaO	19.02	2.21	11.58	5.15	-	3.09
Na_2O	0.12	0.01	2.99	2.23	1.54	7.39
K_2O	0.01	0.02	0.22	4.63	12.58	0.35
F	-	-	0.50	-	-	-
Cl	-	-	0.10	-	-	-
Total	100.96	100.95	98.26	95.27	91.71	100.64

1. High-Ca pyrozene, 2. Low-Ca pyroxene, 3. Kaersutite, 4. Ca-Na rich glass, 5. K-rich glass, 6. Na-rich glass.

* Total iron given as FeO.

Kaersutite contains 0.5 wt% F and 0.1 wt% Cl.

Kaersutite structural formula: $Na_{0.88}$ ($Mg_{2.5}1Fe_{1.32}Al_{0.63}Ti_{0.81}$) $Si_{5.92}Al_{2.08}O_{23.53}$ ($OH_{0.2}F_{0.24}Cl_{0.03}$).

Table 2. Chemical compositions of constituent minerals in the multi-crystalline magmatic inclusion (MI-C) in Chassigny olivine.

	MI-C						
	1	2	3	4	5	6	7
SiO_2	46.99	48.96	52.38	71.08	71.20	52.86	75.95
TiO_2	1.96	1.36	0.66	0.30	0.16	0.07	0.24
Al_2O_3	7.07	5.74	3.38	16.17	16.13	29.11	17.67
Cr_2O_3	0.01	0.27	0.23	0.02	0.05	0.08	0.05
FeO*	9.73	6.51	16.81	0.35	0.19	0.06	0.06
MnO	0.21	0.23	0.52	-	0.05	-	-
MgO	10.63	12.96	24.42	0.05	0.08	0.05	0.00
CaO	22.02	20.36	1.15	0.29	3.62	12.65	0.36
Na_2O	0.32	0.64	0.00	5.31	4.48	4.18	2.57
K_2O	0.00	0.04	0.02	6.54	3.54	0.22	0.04
Total	98.95	97.09	99.57	100.11	99.49	99.28	96.94

1. Core of high-Ca pyroxene having reverse zoning, 2. Rim of high-Ca pyroxene having reverse zoning, 3. Low-Ca pyroxene, 4. Na-K rich glass, 5. Ca-Na-K rich glass, 6. Ca-rich glass, 7. Si-rich glass. * Total iron given as FeO.

Ilmenite was found only in one inclusion (MI-C). No polyphase inclusions contain ilmenite coexisting with kaersutite, although both minerals are Ti-rich minerals.

The groundmass in the polyphase inclusion with kaersutite (MI-A) consists of only Ca-Na rich glass that surround the crystals. The glass areas occupy up to 50% of the area exposed in the inclusion. The groundmass in another polyphase inclusion with

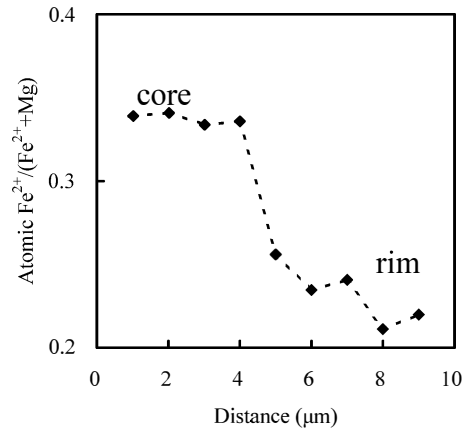

Fig. 2. Zoning profile of the Fe# of high-Ca pyroxene having reverse chemical zoning in a Chassigny magmatic inclusion (MI-C). Each analysis is given in Table 3.

Table 3. Chemical compositions of reverse zoned augite in the multi-crystalline magmatic inclusion (MI-C) in Chassigny olivine.

	core 1	core 2	core 3	core 4	rim 1	rim 2	rim 3	rim 4	rim 5
SiO_2	46.99	47.12	47.03	47.13	49.31	49.57	49.18	50.19	48.96
TiO_2	1.96	1.69	1.51	1.96	1.29	1.29	1.33	1.36	1.36
Al_2O_3	7.07	6.87	6.73	7.16	5.04	4.11	4.52	5.95	5.74
Cr_2O_3	0.01	0.03	0.06	0.06	0.20	0.34	0.47	0.31	0.27
FeO*	9.73	9.12	9.53	9.47	8.00	7.77	7.72	6.51	6.51
MnO	0.21	0.27	0.27	0.24	0.33	0.33	0.26	0.24	0.23
MgO	10.63	9.88	10.67	10.50	13.05	14.21	13.65	13.65	12.96
CaO	22.02	22.07	22.07	22.08	20.69	19.48	20.60	20.10	20.36
Na_2O	0.32	0.26	0.30	0.31	0.31	0.27	0.35	0.60	0.64
K_2O	0.00	0.02	0.00	0.01	0.00	0.02	0.02	0.00	0.04
total	98.95	97.32	98.15	98.92	98.21	97.39	98.10	98.91	97.09
O=	12.00	12.00	12.00	12.00	12.00	12.00	12.00	12.00	12.00
Si	3.58	3.64	3.61	3.59	3.73	3.77	3.73	3.73	3.72
Al	0.42	0.36	0.39	0.41	0.27	0.23	0.27	0.27	0.28
ΣT	4.00	4.00	4.00	4.00	4.00	4.00	4.00	4.00	4.00
Al	0.22	0.26	0.22	0.23	0.18	0.14	0.13	0.25	0.24
Ti	0.11	0.10	0.09	0.11	0.07	0.07	0.08	0.08	0.08
Fe	0.62	0.59	0.61	0.60	0.51	0.49	0.49	0.40	0.41
Cr	0.00	0.00	0.00	0.00	0.01	0.02	0.03	0.02	0.02
Mn	0.01	0.01	0.01	0.01	0.02	0.02	0.01	0.01	0.01
Mg	1.21	1.14	1.22	1.19	1.47	1.61	1.54	1.51	1.47
Ca	1.80	1.83	1.82	1.80	1.68	1.59	1.67	1.60	1.66
Na	0.05	0.04	0.04	0.05	0.04	0.04	0.05	0.09	0.09
K	0.00	0.00	0.00	0.00	0.00	0.00	0.00	0.00	0.00
Σcation	8.01	7.97	8.02	8.00	7.99	7.98	8.01	7.97	7.98
Fe#	0.34	0.34	0.33	0.34	0.26	0.23	0.24	0.21	0.22

* Total iron given as FeO.

kaersutite (MI-B) consists of three different glass phases, that are Ca-Na rich glass, sanidine-composition glass and albite-composition glass. The groundmass in MI-C consists of four different types of glasses (Table 2).

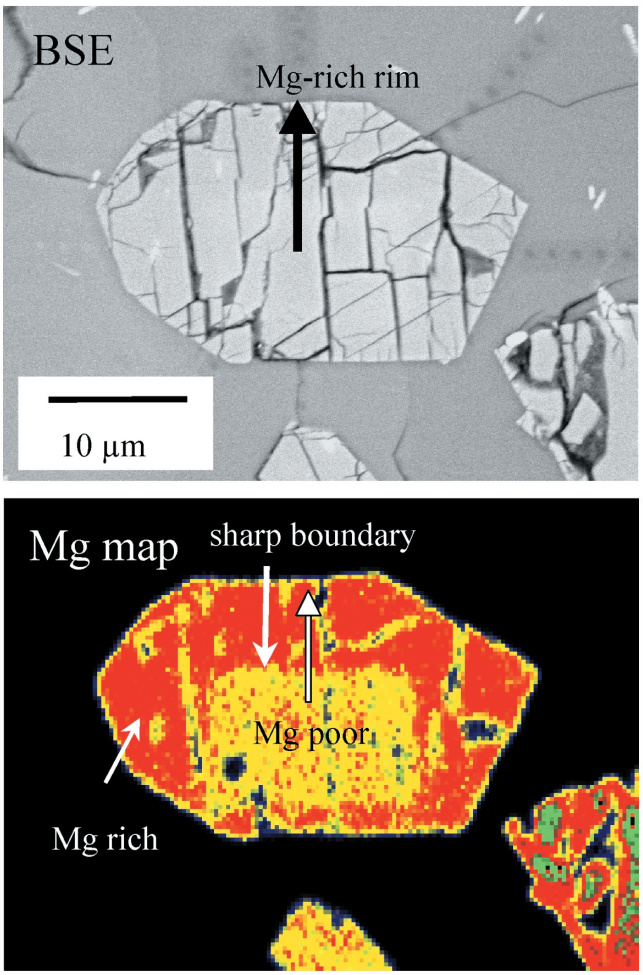

Fig. 3. BSE image and Mg X-ray map of high-Ca pyroxene having reverse zoning in a Chassigny magmatic inclusion (MI-C). This grain is located lower left of the MI-C in Fig. 1c. It is about 45° rotated compared to Fig. 4.

3.2. Nakhla

Nakhla is an olivine-bearing clinopyroxenite with the modal abundances of ~80% augite, ~5% olivine, and ~15% fine-grained mesostasis. Most olivine grains occur as subhedral grains, commonly 1–1.5 mm in size, which usually contain magmatic inclusions.

Trapped magmatic inclusions are present near the centers of large olivine grains in Nakhla. Harvey and McSween (1992) reported two distinct textures (polyphase and monocrystalline) of magmatic inclusions in Nakhla. There are no radial cracks around the inclusions (Fig. 4). We observed two magmatic inclusions in two thin sections of Nakhla. Constituent minerals in these inclusions are similar to those previously reported (Harvey and McSween 1992; Treiman, 1993). Polyphase inclusions of

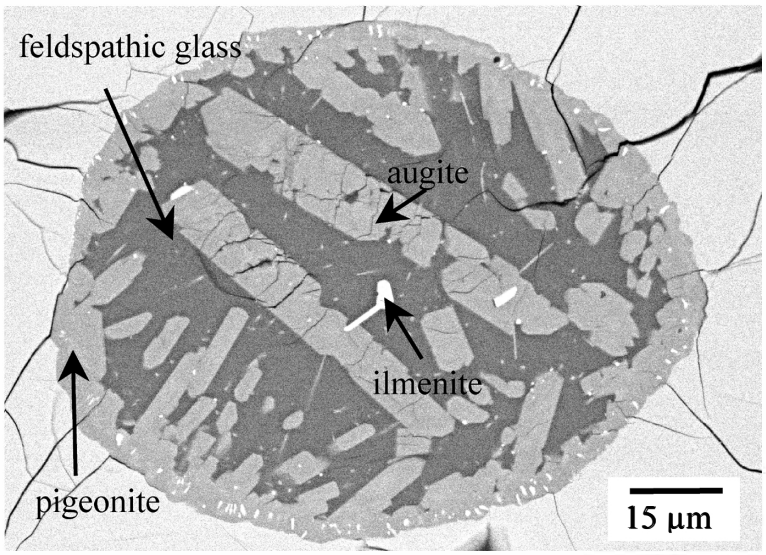

Fig. 4. BSE image of a polyphase inclusion in Nakhla.

euhedral to subhedral crystals in a glassy groundmass have variable sizes (50–400 μm in diameter). They also consist of feldspathic glass, augite, low-Ca pyroxene, alkali feldspar, ilmenite and Ti-magnetite (Harvey and McSween 1992; Treiman 1993) (Fig. 4). Table 2 shows chemical compositions of constituent minerals in the polyphase magmatic inclusion in Nakhla olivine.

Both high-Ca and low-Ca pyroxenes are present in the polyphase inclusions. High-Ca pyroxene is higher in Ti and Al contents (TiO_2=1–1.5 wt%, Al_2O_3=4.5–5.5 wt%) than cumulus augite. The Fe# of the high-Ca pyroxenes are ~0.58. Low-Ca pyroxenes coexist with high-Ca pyroxene. The CaO contents of low-Ca pyroxenes are ~2.2 wt%, showing that low-Ca pyroxenes in polyphase inclusions have very low wollastonite contents (~5%). The Fe# of the low-Ca pyroxenes are ~0.57$\pm$0.1. The $[Fe^{2+}/(Fe^{2+}+Mg)_{CPX}]/[Fe^{2+}/(Fe^{2+}+Mg)_{OPX}]$ ratio (Fe-Mg partition coefficient) is 0.95, showing that high-Ca pyroxenes tend to be slightly more Mg-rich than low-Ca pyroxenes at equilibrium. Thus, low-Ca pyroxenes are in equilibrium with high-Ca pyroxene in Nakhla polyphase inclusions.

The opaque phases in the polyphase inclusions are mostly FeTi oxides (ilmenite and Ti-magnetite). Ilmenite has 44.5 wt% TiO_2, 45 wt% FeO and 2.5 wt% MgO. Ti-magnetite has 14 wt% TiO_2, 75 wt% FeO and 7 wt% Al_2O_3. The FeTi oxides are enclosed in high-Ca pyroxene, showing that the FeTi oxides crystallized before high-Ca pyroxene crystallized. Minute elongate wisps of Ti-Al chromite are present in high-Ca pyroxene nearest to the host olivine at the inner edges of the inclusion. Ti-Al chromite has 10 wt% TiO_2, 60 wt% FeO and 22 wt% Cr_2O_3.

The glass phase in the Nakhla polyphase inclusion is homogeneous and occupies up to 50% of the area exposed in the inclusion. The chemical composition of the glass is rich in Si (SiO_2=~70 wt%) and Al (Al_2O_3=~15 wt%) with ~3.5 wt% CaO, ~3 wt% Na_2O, and ~5.3 wt% K_2O.

4. Discussion

4.1. Crystallization process of the Chassigny magmatic inclusions with high-Ca pyroxene showing reverse zoning

Although augite, which grew during cooling, shows normal zoning from the Mg-rich core to the Mg-poor rim, some Al-, Ti-rich augite grains in the Chassigny magmatic inclusion show reverse zoning from the Mg-poor core to the Mg-rich rim. This means that Chassigny augite experienced some unusual crystallization history, and which can give important constraints on crystallization and formation of the meteorite. Because no report has been done for the presence of reversely-zoned augite in the Chassigny magmatic inclusion, this will provide better and new understanding of the formation of this cumulate rock. The reversely-zoned augite has a sharp boundary between the Mg-poor core and the Mg-rich rim. This observation is important because such a sharp boundary would not be present if reversely-zoned augite has formed by solid state diffusion. There is a possibility that such zoning is due to sector zoning of augite. The sector zoning typically occurs as well developed (010), (100), (111) and (110) sectors which grew at different rates (Brophy *et al*., 1999). The difference in the growth rate can produce apparent reversely-zoned augite having a sharp boundary. If the reversely-zoned augite occurred as sector-zoning, the crystal orientation of the Mg-poor core in the reversely-zoned augite should differ from that of the Mg-rich rim. However, according to observation under crossed Nicol of polarized light microscope, the Mg-poor core region in the reversely-zoned augite has the same extinction angle as the Mg-rich rim region. This indicates that the Mg-poor core region in the reversely-zoned augite has the same crystal orientation as the Mg-rich rim region. Therefore, the formation of reversely-zoned augite in the Chassigny magmatic inclusion must imply that the crystallization stage of the Mg-poor core was different from that of the Mg-rich rim. The compositional relationship between the Chassigny host olivine and the Mg-rich rim of the augite in the Chassigny magmatic inclusion suggests that the Mg-rich rim of the augite is in Fe-Mg equilibrium with the host olivine. In contrast, the Mg-poor core of the reversely-zoned augite in the Chassigny magmatic inclusion is not in equilibrium with the host olivine. Although distribution coefficient (K_D) between augite and olivine depends on Fe# of olivine, temperature and pressure (Kawasaki and Ito, 1994), the K_D is less than 1 when Fe# of Chassigny olivine is 0.32 (Table 4). We also confirmed that the host olivine is in equilibrium with the rim of reversely-zoned augite, not the core by QUILF calculation (Andersen *et al*., 1993). Therefore, the Mg-poor core is considered to be in equilibrium with more Fe-rich olivine compared to the Chassigny host olivine.

Because reversely-zoned augite seems to have formed under a different condition, perhaps the melt that crystallized the Mg-poor core of the augite was different from that which crystallized the Mg-rich rim of the augite. This would require that the melt composition of the Chassigny magmatic inclusion containing reversely-zoned augite changed from Mg-poor to Mg-rich after the formation of the Mg-poor core of augite. There are a few possibilities. This compositional change can be produced by addition of Mg-rich melt. However, it is unlikely that another melt was injected into the magmatic inclusion because the constituent minerals in the magmatic inclusion seem to

Table 4. Distribution coefficient (K_D) between olivine and clinopyroxene.

	K_D	Reference
Experiment		
$T=1215$℃, 0.1 MPa	0.68	Longhi and Pan (1989)
$T=1300$℃, 7.5 MPa	0.78	Kawasaki and Ito (1993)
Host olivine and reverse-zoned augite in Chassigny magmatic inclusion		
Mg-poor core	1.14	
Mg-rich rim	0.71	
Augite in Nakhla magmatic inclusion		
	0.67	

have crystallized under closed system conditions. Instead, we suggest that the compositional change of the magmatic inclusion was produced by melting of the surrounding olivine. The magmatic inclusion (or trapped magma) could melt the surrounding olivine due to change of the *P-T* conditions.

According to this scenario, a crystallization process of the Al-, Ti-rich augite with reverse zoning in the Chassigny magmatic inclusion is as follows (Fig. 5). (a) Chassigny olivine trapped melt during its crystallization. (b) Olivine grew on the host olivine wall after the host olivine trapped the melt as magmatic inclusion. Then, the melt composition became Mg-poor by the growth of olivine because Mg in the melt is consumed by the olivine growth. (c) Mg-poor augite crystallized from such Mg-poor melt. (d) At the next stage, the host olivine became homogeneous because of atomic diffusion between the wall olivine and the host olivine during cooling. Fe# of the bulk magmatic inclusion was different from that of the wall olivine because Mg content of wall olivine changed from Mg-poor to Mg-rich by diffusion event of olivine. (e) Mg-rich melt was produced by the melting of wall olivine that occurred by the change of conditions such as temperature and pressure. (f) Mg-rich augite and orthopyroxene crystallized from the Mg-rich melt. Then, the Mg-rich rim formed surrounding the Mg-poor augite that crystallized during the first stage. Such a process could form reverse zoning of augite. This scenario is supported by heating experiments of magmatic inclusion in magnesian olivine (Danyushevsky *et al*., 2000). Danyushevsky *et al*. (2000) reported a re-equilibration process of magmatic inclusions in olivine phenocrysts. They suggested that the composition of magmatic inclusion changes by the degree of re-equilibration. Fe# of magmatic inclusion modified by partial re-equilibration is lower than the initial Fe# due to crystallization of wall olivine. The stage (b) of Fig. 5 is consistent with this result. Fe# of magmatic inclusion modified by complete re-equilibration is as much as the initial Fe#, and Fe# of wall olivine is also as much as that of the host olivine. These seem to be due to atomic diffusion during the complete re-equilibration process. The stage (d) of Fig. 5 seems to be supported by this result.

4.2. Comparison of magmatic inclusions between Chassigny and Nakhla

In order to further discuss the formation process of Al-, Ti-rich augite having

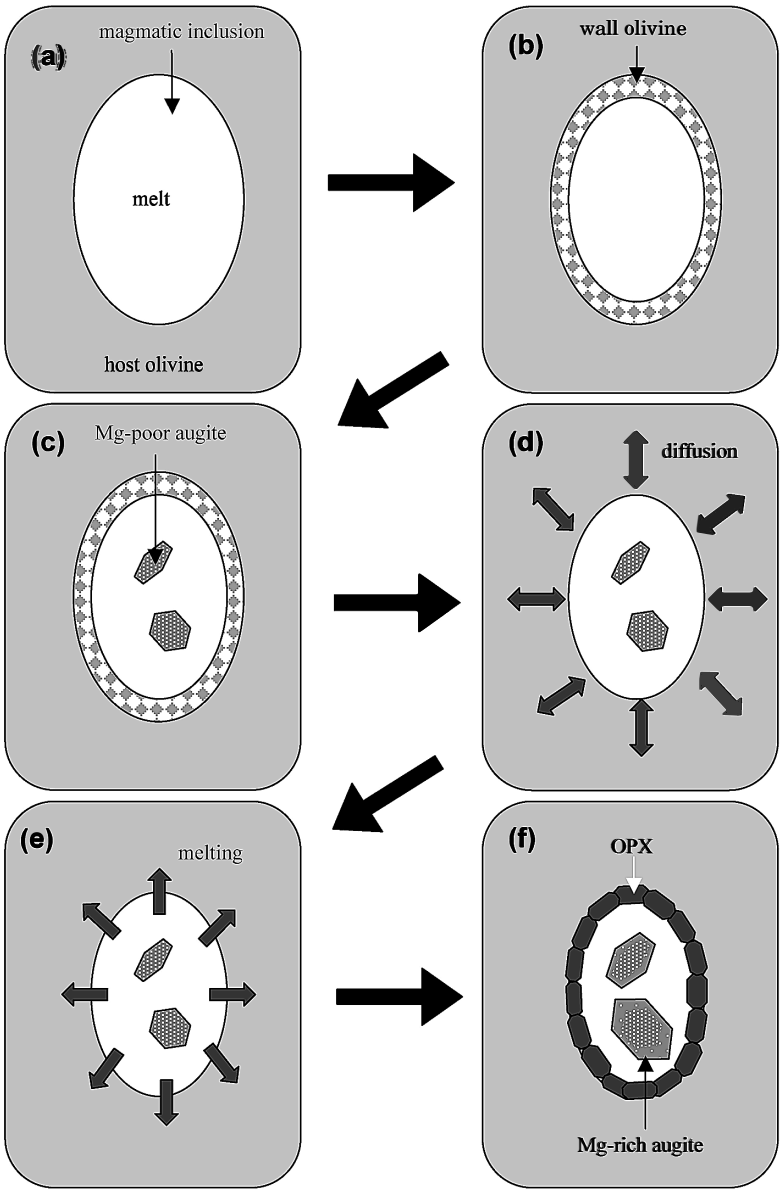

Fig. 5. Hypothetical crystallization process of augite with reverse zoning. (a) Chassigny olivine trapped melt during its crystallization. (b) The melt composition became Fe-rich while olivine grew on the host olivine wall. (c) Mg-poor augite crystallized from Fe-rich melt. (d) The host olivine became homogeneous because of atomic diffusion between the wall olivine and the host olivine during cooling. (e) Mg-rich melt was produced by melting of wall olivine that occurred by the change of conditions such as temperature and pressure. (f) Mg content in the melt increased and Mg-rich augite and orthopyroxene (opx) crystallized from the Mg-rich melt.

reverse zoning in the Chassigny magmatic inclusion, we compare the observation results of Chassigny magmatic inclusions with those of Nakhla magmatic inclusions. We proposed that the Mg-rich rim of such Al-, Ti-rich augite in the Chassigny magmatic inclusion grew during re-melting of the magmatic inclusion. This re-melting process can be explained by some possibilities. Chassigny magmatic inclusions may be re-melted while host rock was trapped by other magma. If the inclusions have melted by this process, the Mg-poor augite core would completely melt because high temperature was kept for a long time. Therefore, this process is unlikely. High temperature should be kept only for a short time because the Mg-poor augite core remained without melting. This condition is consistent with the rapid cooling induced by an impact event. If this is the case, the observation that there is no reverse zoning of high-Ca pyroxene in Nakhla magmatic inclusions is reasonable, showing that Nakhla magmatic inclusions have not experienced a re-melting process.

Re-melting by an impact event is also supported by the presence of radial cracks in Chassigny magmatic inclusions (Fig. 1). Chassigny magmatic inclusions have many radial cracks around them. Although cracks around magmatic inclusions could be formed by the fracturing of a phenocryst induced by rapid compression and decompression or thermal shock within the inclusion (Wallace and Gerlach, 1994), radial cracks around Chassigny magmatic inclusion seem to have formed by homogeneous expansion of the inclusion. Thus, the formation of such radial cracks is most likely due to reheating by an impact event after the formation of the inclusion. The occurrence of homogeneous expansion seems to be induced by rapid compression-expansion that occurred during an impact event.

The above hypothesis is supported by the difference of the shock pressure that Nakhla and Chassigny have experienced. Chassigny is estimated to have experienced a shock pressure reaching 35 GPa (Langenhorst and Greshake, 1999). Chassigny magmatic inclusions seem to have expanded by high pressure induced by an impact event. The expansion of their inclusions seems to have formed radial cracks in Chassigny. In contrast, Nakhla magmatic inclusions have less cracks and do not have radial cracks. Nakhla has been only mildly shocked with an estimated peak pressure of about 20 GPa (Greshake and Langenhorst, 1997). The reason of the absence of radial cracks around Nakhla magmatic inclusions is because Nakhla magmatic inclusions have not expanded too much due to a relatively weak shock pressure. Radial cracks are not present around terrestrial magmatic inclusion because terrestrial magmatic inclusions have not experienced impact events. We suggest that Chassigny magmatic inclusions have been affected by a heavy impact event, producing reverse zoning of Al-, Ti-rich augite.

It is not clear why two types of inclusions (reversely-zoned augite-bearing and reversely-zoned augite-free) coexist in Chassigny magmatic inclusions. The possible reason is that an impact event partially melted the augite grains in MI-C because this inclusion experienced a higher shock pressure than the other inclusions by some reason. Alternatively, the other inclusions were totally melted and only MI-C experienced partial melting. Because the radial cracks were observed in all magmatic inclusions in Chassigny, the latter will be more likely.

5. Conclusions

(1) Some Al-, Ti-rich augites in Chassigny magmatic inclusions show reverse zoning from the Mg-poor core to the Mg-rich rim. The crystallization stage of the Mg-poor core is different from that of Mg-rich rim because the zoned augite has a sharp boundary between the Mg-rich and Mg-poor regions.

(2) The formation of reverse zoning of augite in the Chassigny magmatic inclusions can be explained by re-melting of the inclusions induced by a shock event.

(3) Chassigny magmatic inclusions have many radial cracks around them because magmatic inclusions in olivine of Chassigny are probably reheated by an impact event after the formation of the inclusion. In contrast, Nakhla magmatic inclusions have less cracks because Nakhla has been only mildly shocked.

(4) Constituent minerals in Chassigny magmatic inclusions seem to have crystallized from the melt having distinct composition from the Chassigny parent magma and under different conditions from that magmatic inclusion was originally trapped in olivine grains. Therefore, it is unlikely that constituent minerals in Chassigny magmatic inclusions directly represent minerals that crystallized from the Chassigny parent magma.

Acknowledgments

We would like to acknowledge Dr. A. Greshake (Natural History Museum of Berlin), the Smithsonian Institution, and the University of Hawaii for the loan of the Chassigny thin sections. We thank Dr. T. Ishii (Ocean Res. Inst., University of Tokyo) for discussion and providing technical support during the electron microprobe analysis. Constructive reviews by Drs. A. Treiman, H. Nekvasil and Y. Ikeda greatly improved the quality of the manuscript.

References

Anderson, D.J., Lindsley, D.H. and Davidson, P.M. (1993): QUILF: A Pascal program to assess equilibria among Fe-Mg-Mn-Ti oxides, pyroxenes, olivine and quartz. Computers Geosci., **19**, 1333–1350.

Bogard, D.D. and Johnson, P. (1983): Martian gases in an Antarctic meteorite. Science, **221**, 651–654.

Brophy, J.G., Whittington, C.S. and Park, Y.R. (1999): Sector-zoned augite megacrysts in Aleutian high alumina basalts: implications for the conditions of basalt crystallization and the generation of calc-alkaline series magmas. Contrib. Mineral. Petrol., **135**, 277–290.

Danyushevsky, L.V., Della-Pasqua, F.N. and Sokolov, S. (2000): Re-equilibration of melt inclusions trapped by magnesian olivine phenocrysts from subduction-related magmas: Petrological implications. Contrib. Mineral. Petrol., **138**, 68–83.

Floran, R.J., Prinz, M., Hlava, P.F., Keil, K., Nehru, C.E. and Hinthorne, J.R. (1978): The Chassigny meteorite: a cumulate dunite with hydrous amphibole-bearing melt inclusions. Geochim. Cosmochim. Acta, **42**, 1213–1229.

Greshake, A. and Langenhorst, F. (1997): TEM characterization of shock defects in minerals of the martian meteorite Chassigny. Meteorit. Planet. Sci., **32** (Suppl.) A52.

Harvey, R.P. and McSween, H.Y., Jr. (1992): Petrogenesis of the nakhlite meteorites: Evidence from cumulate mineral zoning. Geochim. Cosmochim. Acta, **56**, 1655–1663.

Johnson, M.C., Rutherford, M.J. and Hess, P.C. (1991): Chassigny petrogenesis: Melt compositions, intensive

parameters, and water contents of Martian (?) magmas. Geochim. Cosmochim. Acta, **55**, 349–366.
Kawasaki, T. and Ito, E. (1993): An experimental determination of the exchange reaction of Fe^{2+} and Mg^{2+} between olivine and Ca-rich clinopyroxene. Am. Mineral., **79**, 461–477.
Langenhorst, F. and Greshake, A. (1999): A transmission electron microscope study of Chassigny: Evidence for strong shock metamorphism. Meteorit. Planet. Sci., **34**, 43–48.
Longhi, J. and Pan, V. (1989): The parent magmas of SNC meteorites. Proc. Lunar Planet. Sci. Conf., **19th**, 451–464.
McSween, H.Y., Jr. (1985): SNC meteorites: Clues to Martian petrologic evolution? Rev. Geophys., **23**, 391–416.
McSween, H.Y., Jr. (1994): What we have learned about Mars from SNC meteorites. Meteoritics, **29**, 757–779.
Treiman, A.H. (1993): The parent magma of the Nakhla (SNC) meteorite, inferred from magmatic inclusion. Geochim. Cosmochim. Acta, **57**, 4753–4767.
Varela, M.E., Kurat, G., Bonnin-Mosbah, M., Clocchiatti, R. and Massare, D. (2000): Glass-bearing inclusions in olivine of the Chassigny achondrite: Heterogeneous trapping at sub-igneous temperatures. Meteorit. Planet. Sci., **35**, 39–52.
Wadhwa, M. and Crozaz, G. (1995): Trace and minor elements in minerals of nakhlites and Chassigny: Clues to their petrogenesis. Geochim. Cosmochim. Acta, **59**, 3629–3645.
Wallace, P.J. and Gerlach, T.M. (1994): Magmatic vapor source for sulfur dioxide released during volcanic eruptions: Evidence from Mount Pinatubo. Science, **265**, 497–499.
Watson, L.L., Hutcheon, I.D., Epstein, S. and Stolper, E.M. (1994): Water on Mars: Clues from deuterium/hydrogen and water contents of hydrous phases in SNC meteorites. Science, **265**, 86–90.
Wood, C.A. and Ashwal, L.D. (1981): Meteorites from Mars: Prospects, problems and implications. Lunar and Planetary Science XII. Houston, Lunar Planet. Inst., 1197–1199.